Heliyon 7 (2021) e07165

Contents lists available at ScienceDirect

Heliyon

journal homepage: www.cell.com/heliyon

Research article

The synthesis and characterization of Fe_2O_3@SiO_2–SO_3H nanofibers as a novel magnetic core-shell catalyst for formamidine and formamide synthesis

Hakimeh Ziyadi [a,*], Mitra Baghali [b], Akbar Heydari [c]

[a] Department of Organic Chemistry, Faculty of Pharmaceutical Chemistry, Tehran Medical Sciences, Islamic Azad University, Tehran, Iran
[b] Department of Chemistry, Faculty of Pharmaceutical Chemistry, Tehran Medical Sciences, Islamic Azad University, Tehran, Iran
[c] Chemistry Department, Tarbiat Modares University, Tehran, Iran

ARTICLE INFO

Keywords:
Core-shell nanofibers
Fe_2O_3@SiO_2–SO_3H
Electrospinning
Nano catalyst
Formamidine
Formamide

ABSTRACT

Over the past several decades, the fabrication of novel ceramic nanofibers applicable in different areas has been a frequent focus of scientists around the world. Aiming to introduce novel ceramic core-shell nanofibers as a magnetic solid acid catalyst, Fe_2O_3@SiO_2–SO_3H magnetic nanofibers were prepared in this study using a modification of Fe_2O_3@SiO_2 core-shell nanofibers with chlorosulfonic acid to increase the acidic properties of these ceramic nanofibers. The products were characterized by scanning electron microscope (SEM), transmission electron microscope (TEM), energy dispersive X-ray spectroscope (EDS), vibrating sample magnetometer (VSM), X-ray diffraction (XRD) and Fourier transform infrared spectroscopy (FT-IR). The prepared nanofibers were used as catalysts in formamide and formamidine synthesis. The treatment of aqueous formic acid using diverse amines with a catalytic amount of Fe_2O_3@SiO_2–SO_3H nanofibers as a reusable, magnetic and heterogeneous catalyst produced high yields of corresponding formamides at room temperature. Likewise, the reaction of diverse amines with triethyl orthoformate led to the synthesis of formamidine derivatives in excellent yields using this novel catalyst. The catalytic system was able to be recovered and reused at least five times without any catalytic activity loss. Thus, novel core-shell nanofibers can act as efficient solid acid catalysts in different organic reactions capable of being reused several times due to their easy separation by applying magnet.

1. Introduction

Over the last decades, the use of Bronsted acid catalysts has been increased in both laboratories and industries processes, such as biodiesel production, esterification and hydrolysis because of liquid phase limitations, hard separation, non-recovery acidic waste generation and the corrosion of reactors [1, 2, 3, 4]. Nano-substrates with a larger surface area and high surface-to-volume ratio have been applied in the solid acid catalysis field to increase available catalytic centers and enhance catalytic activity [5, 6]. Among solid nano catalysts, magnetic core-shell nano catalysts have been widely used because of their easy separation and recovery by applying a magnet as well as functionalization possibilities of the inorganic surface. Magnetic field separation is more effective than conventional separation methods such as purification and centrifuge because it can reduce catalyst waste, optimize operational cost and enhance the purity of products [7, 8, 9, 10]. By choosing the appropriate shell, the functionality of the catalyst in the shell is improved. Besides, this shell prevents the accumulation of magnetic nanostructure and enhances its chemical stability [11].

Iron oxide magnetic core-shell nanoparticles have been prepared in various ways and have been modified by functional groups with catalytic properties [12]. Silica is one of the best coatings used for the synthesis of iron oxide core-shell nanoparticles because of stability, biocompatibility, functionality and resistance to acid or high temperature [13, 14]. The acid catalytic properties of iron oxide@SiO_2 nanoparticles can be exceeded by the modification of the surface of nanoparticles with acid functional groups, such as HBF_4 [15], sulfuric acid [16], R-$NHMe_2$] [H_2PO_4] [17] and sulfonic acid [18]. Solid acid catalyst functionalized with sulfonic acid could be used in different organic reaction [19, 20, 21]. The iron oxide coated with silica and functionalized with sulfonic acid (Fe_3O_4@SiO_2–SO_3H) nanoparticles has been used as an effective catalyst in the synthesis of pyrimidinones [22], pyrazole [23], quinoline [24], pyrazolopyridines [25] and dihydropyrimidinones/thiones [26] as well as in the reduction of oximes to amines [27] and esterification reactions [28]. However, all the above-mentioned catalysts are

* Corresponding author.
E-mail address: behnazziyadi@yahoo.com (H. Ziyadi).

https://doi.org/10.1016/j.heliyon.2021.e07165
Received 9 February 2021; Received in revised form 29 April 2021; Accepted 26 May 2021

nanoparticles as a zero-dimensional nanostructure. It seems that the use of other nanostructures with different morphology (such as one-dimensional nanostructure) as a catalyst in organic reaction is very limited and needs further study.

Nanofibers are a new generation of one-dimensional nanostructures frequently used for their different applications like filtration [29], membrane [30], sensor [31], food and packaging [32], medical applications [33] and catalysis [34]. Electrospinning followed by calcination provides a tunable, simple and versatile way for generating ceramic nanofibers with unique properties including high surface area, large porosity, mechanical roughness, superb thermal stability, higher electron transfer and enhancement of the thermo electric merit and magnetic moment [35]. Such new properties lead to the potential application of ceramic nanofibers in lithium batteries, data storage devices, magnetic resonance imaging, sensing devices, energy storage, targeted drug delivery and catalysis [36, 37, 38]. Recently, some researchers have focused on the fabrication of porous ceramic nanofibers and their applications in heterogeneous reactions [39]. Pd–TiO_2 nanofibers have been applied in Suzuki coupling reaction with high conversion efficiency due to their high surface area and larger number of active sites [40]. $Cu_{25}O/Ni_{75}O$ nanofibers can be used as anode catalysts for hydrazine oxidation in alkaline [41]. In one study, Pt/TiO_2 nanofibers were used during electrochemical reaction for methanol oxidation and were found to effectively facilitate electron transport [42]. In another study, Pt supports composed of graphene sheets decorated by Fe_2O_3 nanorods and denoted as Pt/Fe_2O_3/N-RGO displayed higher catalytic activity than free Pt in the 4-nitrophenol hydrogenation reaction [43]. Previously, our research group prepared iron oxide nanofibers and applied them as catalysts in alcohol oxidation [44] and methyl orange degradation as a Fenton catalyst [45]. Also, in other studies, our group examined the fabrication and catalytic application of core-shell Fe_2O_3@SiO_2 nanofibers as novel magnetic nanofibers for the one-pot reductive amination of carbonyl compound [46, 47]. It seems that by functionalization of the surface of Fe_2O_3@SiO_2 nanofibers, this magnetic solid nano catalyst can be used in various organic reactions.

Formamides are important crossroad intermediates in organic component synthesis such as formamidines [48], isocyanides [49], Vilsmeier reagents [50], fluoroquinolones [51] and imidazoles [52]. Hence, researchers have focused on the synthesis of formamides via the reaction of amines with various N-formylating agents such as carbon dioxide [53, 54], phenyl chloroformate [55], methyl formate [56], ammonium formate [57] and acetic formic anhydride [58]. Of these reagents, formic acid as a cheap, non-toxic, stable formylating compound is a good candidate for N-formylating amines. Unfortunately, their moderate reactivity demands increased reaction temperatures or catalyst presence, particularly for aromatic and sterically-hindered amines formylation. So, formic acid has been used in the presences of catalysts such as poly ethylene glycol [59], zeolite [60], ZnO [61], $ZnCl_2$ [62], thiamine hydrochloride [63] and cobalt nanoparticles [64]. Nishikawa et al. studied the synthesis of *N*-formamides with formic acid under mild conditions using tetraethylorthosilicate (TEOS) [65]. However, a long reaction time requires a Dean-Stark trap in reflux conditions and the difficult N-formylation of electron-withdrawing derivatives of anilines can limit the usage of these catalysts. Besides, the above-mentioned catalyst recycles need to be centrifuged or a long-time filtration leading to the unavoidable loss of solid catalyst in the process of separation. Thus, it seems that magnetic nanostructures modified with silica and reinforced with an acid functional group can be a good choice as a catalyst for N-formylation.

Formamidines are widely used as effective drug agents and useful intermediate in the synthesis of purine [66] imidazole and quinazoline [67] compounds. Formamidines and related anions can bind transition metals. Recently, formamidines derivatives with Ni (II) [68] Au (I), Ag (I) [69] Co (II) [70] Cu (II) [71] Pt [72] and Pd [73] ions have been synthesized. Amidine functional group has various biological properties, such as anti-virus [74], anti-AIDS [75], anti-degenerative [76], anticancer [77], anti-platelet [78] and antimicrobial [79] activities. Finding simple and moderate conditions for the synthesis of formamidine can be useful in the production of many organic compounds.

Continuing our previous research [44, 45, 46, 47], this study sought to prepare Fe_2O_3@SiO_2–SO_3H nanofibers and study their use as a heterogeneous acid catalyst in organic reactions aiming at introducing a new generation of one-dimensional nano catalysts in organic reactions. For this purpose, iron oxide nanofibers, prepared by a combination of electrospinning and calcinations, were coated with silica using tetraethyl orthosilicate. Next, the silica surface was reacted with chlorosulfonic acid to obtain Fe_2O_3@SiO_2–SO_3H nanofibers. Due to the significance of formamide group, we decided to examine the catalytic performance of Fe_2O_3@SiO_2–SO_3H nanofibers as a novel magnetic nano catalyst in the N-formylation of amines using formic acid. We also decided to study the catalytic ability of Fe_2O_3@SiO_2–SO_3H nanofibers in the synthesis of formamidine via the reaction of different amines with triethyl orthoformate as a second catalytic reaction.

2. Experimental

2.1. Materials

Poly (vinyl alcohol) (PVA) of 88,000 g/mol molecular weight and 88% degree of hydrolysis were obtained from Sigma-Aldrich (USA). The chemicals used in the study were all purchased from Merck Company. No further purification was done to the reagents with deionized water used as a solvent.

2.2. Preparation of Fe_2O_3@SiO_2–SO_3H nanofibers

2.2.1. Preparation of Fe_2O_3@SiO_2 nanofibers

Fe_2O_3@SiO_2 nanofibers were prepared based on the method employed in our previous study [46]. In summary, 10 ml of 8% W/W PVA solutions were prepared in deionized water as a solvent. Then, 2 g ferric nitrate ($Fe(NO_3)_3.9H_2O$) was added and stirred for 1 h at room temperature. The electrospinning process was conducted by Electroris (FNM Ltd., Iran, http://www.fnm.ir) that as an electrospinning device can control electrospinning parameters such as high voltage (1–35 kV), injection rate with syringe pump (0.1–100 mL/h), drum rotating speed (0–1000 rpm), drum-to-nozzle distance (0–300 mm), needle scanning rate (0–100 mm/min) and the electrospinning media temperature. The electrospinning condition of the prepared solutions was as follows: 5ml syringe with an 18-gauge needle as a nozzle, a rotating drum with 300 rpm speed covered with an aluminum foil as a collector, the applied voltage of 20 kV, 2 ml/h for the rate of injection and 12 cm for the distance between the collector and nozzle. Next, the electrospun PVA/$Fe(NO_3)_3.9H_2O$ nanofibers were peeled off from foil and then calcinated at 600 °C for 6 h to entirely eliminate the organics with the heating rate of 20 °C/min, which produced iron oxide (Fe_2O_3) nanofibers.

In the next step for coating with SiO_2, a mixture of ethanol (15ml), deionized water (5ml) and aqueous ammonia solution (1 ml, 25 wt%) were obtained and stirred completely; then 25 mg of obtained Fe_2O_3 nanofibers were added to this mixture and stirred at room temperature. Then, the solution of 30 ml ethanol and 1 ml tetraethyl orthosilicate (TEOS) were mixed with dispersed Fe_2O_3 nanofibers using a syringe pump. Finally, after relaxation for 6 h, the core-shell nanofibers were separated using a super magnet and washed with ethanol and deionized water.

2.2.2. Functionalization of nanofibers surface with sulfonic acid

200 mg of Fe_2O_3@SiO_2 nanofibers were added into the mixture of diethyl ether (1 ml) and chlorosulfonic acid (0.6 ml) and stirred for 3h at room temperature until the release of hydrochloric acid gas was stopped. The residue was washed with diethyl ether and deionized water and dried for 6h at 100 °C in an oven to obtain the desired nanofibers.

2.2.3. Determination of the amount of acid on the nanofibers

The amount of acid on nanofibers was determined using titration with base. For each titration operation, 50 mg of nanofibers was weighed and transferred to a beaker. Then, 2 ml from potassium hydroxide 0.1 M was added. The prepared suspension was stirred by a magnetic stirrer for 15 min. Then, the nanofibers were separated by a magnet, and the clear solution was titrated with 0.1 M hydrochloric acid in the presence of phenolphthalein.

2.3. Characterization

The characterization of obtained products was carried out using scanning electron microscope (SEM), energy dispersive x-ray spectroscopy (EDS), transmission electron microscope (TEM), X-ray diffraction (XRD), Fourier transform infrared spectroscopy (FT-IR) and, vibrating sample magnetometer (VSM). SEM images were observed using SEM (PhilipsXL30 and S-4160) with gold coating equipped with EDS. TEM measurements were done at 120 kV (Philips, model CM120). Powder XRD spectrum was recorded at room temperature by a Philips X'pert 1710 diffractometer using Cu Kα (α¼ 1.54056 Å) in Bragg-Brentanogeometry (θ-2θ). FT-IR spectra were obtained over the region 400–4000 cm^{-1} with NICOLETIR 100 FT-IR and spectroscopic grade KBr. The magnetic properties of catalyst were attained by Vibrating Sample Magnetometer/Alternating Gradient Force Magnetometer (VSM/AGFM, MDK Co., Iran, http://www.mdk-magnetics.com).

2.4. Synthesis of formamidine derivatives from amines

For each reaction, 1 mmol of triethyl orthoformate was transferred to a small glass flask. Then, 1 mol% of catalyst (0.01 mmol H^+ in the catalyst, 25 mg Fe_2O_3@SiO_2–SO_3H nanofibers) was added. The obtained mixture was stirred by a magnetic stirrer for 15min. Then, 1 mmol of amine was added slowly to be stirred at room temperature (24–27 °C). The reaction progress was followed by thin-layer chromatography with hexane-ethyl acetate at a ratio of 1:4. After the completion of the reaction, 5 ml of dichloromethane was added, and the catalyst was separated by a magnet. The solvent was evaporated using vacuum distillation. The obtained precipitate in dichloromethane was dissolved and re-crystallized. Then, the isolated product was weighed on an electronic balance and used to compute percent yield based on isolated product weight in terms of the expected weight of the product. The synthesized compounds were identified by FT-IR, Mass and NMR spectroscopy and compared with those reported in the literature. The spectral data for selected products are presented below:

N,N′-Bis-(3,4-dicholoro-phenyl)-formamidine (Table 3, entry 7): White solid, mp 134–135 °C; ^{1}HNMR ($CDCl_3$, 400MHz): δ7.25 (m, 2H), 7.28 (d, J = 6.40 Hz, 1H), 7.41 (br s, 1H), 8.39 (m, 2H), 8.5 (s, 1H), 8.85 (s, 1H).

FTIR: 697 cm^{-1}, 749 cm^{-1}, 820 cm^{-1}, 866 cm^{-1}, 1048 cm^{-1}, 1100 cm^{-1}, 1147 cm^{-1}, 1296 cm^{-1}, 1396 cm^{-1}, 1468 cm^{-1}, 1524 cm^{-1}, 1587 cm^{-1}, 1665 cm^{-1}, 2895 cm^{-1}, 3077 cm^{-1}, 3242 cm^{-1}, 3395 cm^{-1}. MS m/z: 334(M^+).

1H-Benzimidazole (Table 3, **entry 9**): Pale yellow solid, mp 169–170 °C, ^{1}H NMR ($CDCl_3$, 400 MHz): δ7.10–7.23 (m, 2H),7.61–7.64 (m, 2H), 8.17 (s, 1H), 10.31–11.1 (br s, NH).

FTIR: 619 cm^{-1}, 743 cm^{-1}, 876 cm^{-1}, 950 cm^{-1}, 1001 cm^{-1}, 1125 cm^{-1}, 1202 cm^{-1}, 1243 cm^{-1}, 1303 cm^{-1}, 1405 cm^{-1}, 1456 cm^{-1}, 1591 cm^{-1}, 1703 cm^{-1}, 2736 cm^{-1}, 2806 cm^{-1}, 2854 cm^{-1}, 2933 cm^{-1}, 3061 cm^{-1}, 3425 cm^{-1}. MS m/z: 118 (M^+).

2.5. Synthesis of formamide derivatives from amine

10 mg of Fe_2O_3@SiO_2–SO_3H was added to 1.2 mmol aqueous formic acid. After five minutes of stirring, 1.0 mmol of amine was added and the reaction mixture was stirred at room temperature (24–27 °C). The reaction progress was followed by thin-layer chromatography with hexane-ethyl acetate at a ratio of 1:4. After the completion of the reaction, an external magnet was used to separate the catalysts. The reaction mixture was extracted with CH_2Cl_2 and H_2O. The organic layer was then dried over anhydrous Na_2SO_4 and identified bythe^{1}H NMR spectroscopy. The percent yield was calculated by the same procedure as mentioned in section 2.4. The spectral data for selected products are presented below:

4- morpholin carbaldehyde (Table 4, **entry 8**): colorless oil, ^{1}H NMR ($CDCl_3$, 400 MHz): δ3.37 (t, 2H, J = 5.1 Hz), 3.55 (t, 2H, J = 5.1 Hz), 3.62 (t, 2H, J = 5.1 Hz), 3.65 (t, 2H, J = 5.1 Hz), 8.04 (s, 1H).

N-(tert-Butylamine) formamide (Table 4, **entry 6**): colorless oil,^{1} HNMR (400 MHz, $CDCl_3$): 50:50 (cis/trans) δ 1.32 (s, 9H), 7.28 (d, 1H, J = 2.3, *cis*), 7.43 (br, 1H, *cis*), 7.51 (br, 1H, *trans*) 7.67 (d, 1H, J = 12.2, *trans*).

3. Results and discussion

3.1. Preparation of Fe_2O_3@SiO_2–SO_3H nanofibers

The generation of well-controlled ceramic nanofibers is typically conducted as follows: (i) the preparation of an electrospinning solution containing a polymer and sol-gel precursor of the ceramic material, (ii) electrospinning the polymeric solution under appropriate conditions and (iii) the calcination of the polymer/precursor composite nanofibers at high temperature to remove polymers and obtain the ceramic phase [35, 36]. Coaxial electrospinning with two immiscible components or polymer in a core-shell nozzle followed by calcination is a conventional electrospinning method used for fabricating core-shell ceramic nanofibers [39]. However, similar to our previous study [46], in this study one-dimensional Fe_2O_3@SiO_2 nanofibers were prepared by a different and new method with the idea of preparing of Fe_2O_3@SiO_2 nanoparticles using a coating of iron oxide (Figure 1). To do so, first, polymer/precursor composite nanofibers were fabricated by the routine uniaxial electrospinning of PVA polymer containing $Fe(NO_3)_3$ as an iron precursor. Iron oxide nanofibers were then obtained by calcinating polymeric nanofibers. Finally, these nanofibers were coated with silica by the sol-gel method in the vicinity of TEOS. The products of the three

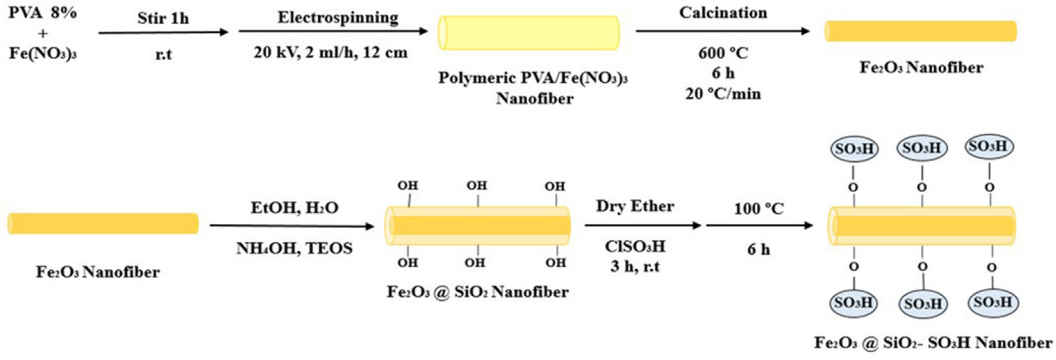

Figure 1. Preparation of Fe_2O_3@SiO_2–SO_3H nanofibers.

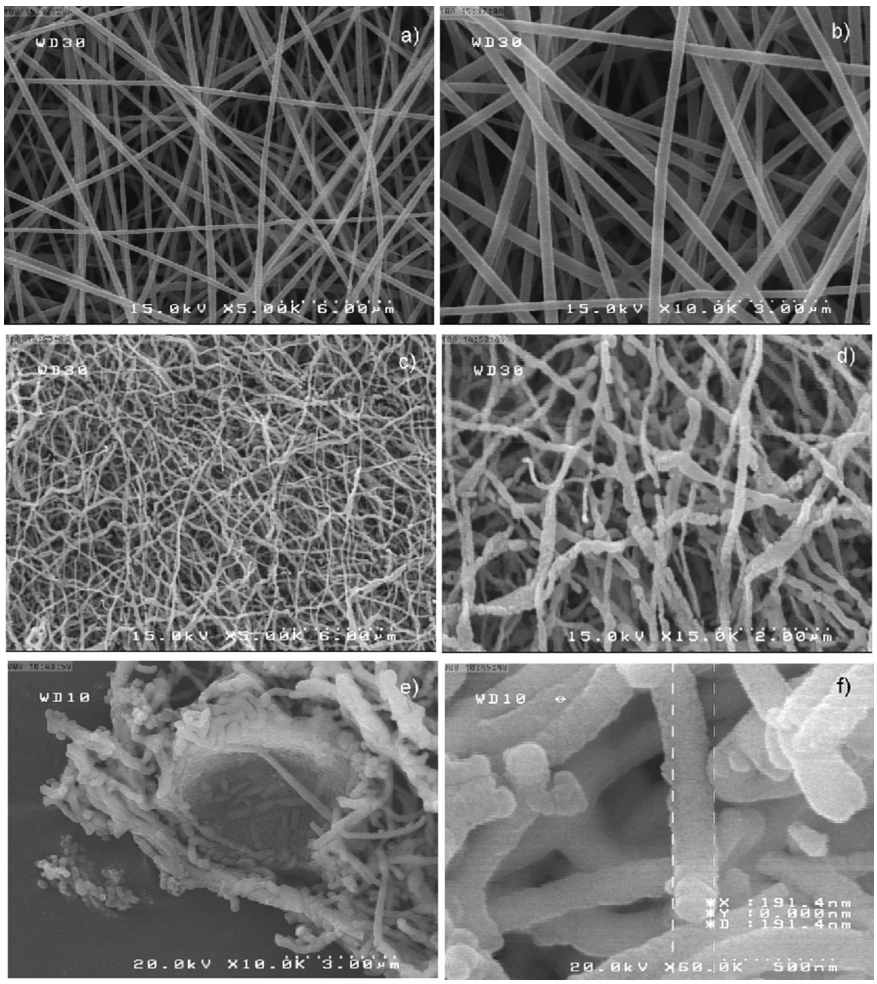

Figure 2. SEM images of a, b) PVA/$Fe(NO_3)_3$ nanofiber c, d) Fe_2O_3 nanofiber e, f) Fe_2O_3@SiO_2 nanofibers with different magnification.

steps were characterized using SEM to approve one-dimensional nanostructure formation.

The SEM images of PVA/$Fe(NO_3)_3$ nanofiber, Fe_2O_3 nanofiber and Fe_2O_3@SiO_2 nanofibers are shown in Figure 2. As can be seen in Figure 2 a, b, the successful electrospinning of PVA/$Fe(NO_3)_3$ solution led to smooth and fine one-dimensional polymeric nanofibers without bead. However, when composite nanofibers were calcinated at high temperature controlled the rising speed, the surface of Fe_2O_3 nanofibers appeared with rough surface, bended shape and a few ruptures in the axial direction (Figure 2 c, d). Finally, as shown in Figure 2 e, f, successful and homogenous coating of iron oxide nanofibers with TEOS produced fine Fe_2O_3@SiO_2 nanofibers. The average diameters of nanofibers were calculated by the measurement software based on 15 fibers at random in SEM image. The average diameters of PVA/$Fe(NO_3)_3$ nanofibers, Fe_2O_3 nanofibers and Fe_2O_3@SiO_2 nanofibers were 198 $\pm$ 20, 93 $\pm$ 16 and 142 $\pm$ 35 nm respectively, confirming that the diameter of composite nanofibers diminished during calcinations and the removal of organic phase whereas the diameters increased with the coating of Fe_2O_3 nanofibers.

Continuing the coating, the functionalization of Fe_2O_3@SiO_2 nanofibers was followed in this study in order to increase the acidity of surface to be used as novel heterogeneous acid catalyst. For this purpose, the silica surface was reacted with chlorosulfonic acid to obtain Fe_2O_3@SiO_2–SO_3H nanofibers. Figure 3 a, b indicates the SEM analysis of Fe_2O_3@SiO_2–SO_3H nanofibers with different magnification. It is observed that nanofibril structures were produced, but some rupture in fibers can be seen due to the increased acidity in the presence of strong acid functional that led to some corrosion in the direction of nanofibers, although the fiber structure with bigger direction than diameter is observable. The mean diameter of Fe_2O_3@SiO_2–SO_3H nanofibers was determined using measurement software and the fiber diameter distribution histogram was drawn by Origin software. As can be seen in Figure 3 c, diameter distribution is between 50 and 300 nm with a mean diameter up to 137 $\pm$ 12 nm for Fe_2O_3@SiO_2–SO_3H nanofibers. The TEM image of Fe_2O_3@SiO_2–SO_3H nanofibers is shown in Figure 3 d. As the TEM image shows, Fe_2O_3 nanofibers were coated with the uniform layer of silica that was functionalized with SO_3H. It is observed that the dense layer of SiO_2–SO_3H as thick as 7 nm exists on the surface of Fe_2O_3 nanofibers. In contrast to Fe_2O_3@SiO_2 nanofibers (15 nm for SiO_2 layer [46]), it seems that the thinner layer of shell surrounded the magnetic core probably as a result of the corrosion of silica surface during the functionalization with chlorosulfonic acid.

In order to determine the elemental composition and confirm the functionalization of nanofibers, Fe_2O_3, Fe_2O_3@SiO_2 and Fe_2O_3@SiO_2–SO_3H nanofibers were evaluated by EDS analysis (Figure 4).

As can be seen, the Fe and O patterns exist as the main elements in the quantitative analysis of the three nanostructures. Furthermore, Si element can be seen in Fe_2O_3@SiO_2 and Fe_2O_3@SiO_2–SO_3H nanofibers patterns. The presence of S in the EDS analysis of Fe_2O_3@SiO_2–SO_3H nanofibers confirmed the successful functionalization of Fe_2O_3@SiO_2 nanofibers surface with sulfonic acid.

Figure 5 shows the FT-IR spectra of PVA/$Fe(NO_3)_3$ nanofibers, Fe_2O_3 nanofibers, Fe_2O_3@SiO_2 nanofibers and Fe_2O_3@SiO_2–SO_3H nanofibers. The FT-IR of PVA/$Fe(NO_3)_3$ nanofibers in Figure 5 a exhibited various transmittance peaks at 1300-1800 cm^{-1} which were attributed to the functional group of PVA. The main peak in 1721 cm^{-1} corresponding to the (C =O) residual from primary vinyl acetate can be seen in Figure 5 a,

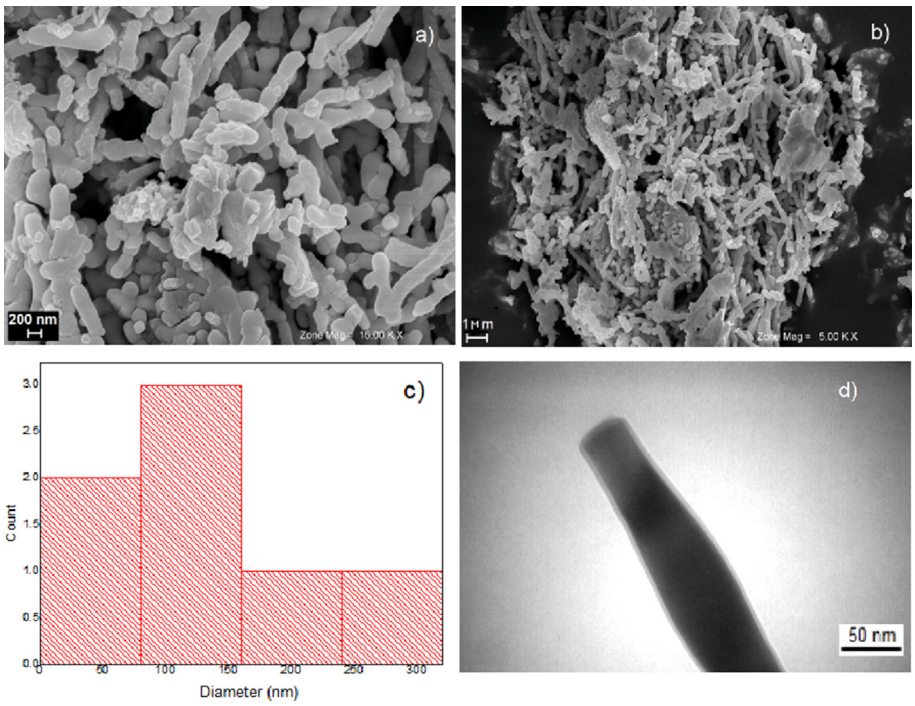

Figure 3. a, b) SEM images with different magnification c) fiber diameter distribution d) TEM image of Fe_2O_3@SiO_2–SO_3H nanofibers.

but this peak decreased significantly in Figure 5 b, c and d due to the removal of PVA during calcinations at high temperature. In Figure 5 b two peaks appeared at 463 and 548 cm^{-1} which could be assigned to the Fe–O vibration of the Fe_2O_3 nanofibers [46] shifting to 461 cm^{-1} and 581 cm^{-1} in Fe_2O_3@SiO_2–SO_3H nanofibers. In all of Fe_2O_3@SiO_2–HA Bronsted acids, the band at 400–650 cm^{-1} is assigned to the stretching vibrations of (Fe–O) bond [15, 80].

The strong peak at 1031 cm^{-1} in Fe_2O_3@SiO_2 nanofibers spectra (Figure 5 c) corresponds to the vibrations of the Si–O bond that appeared as shoulder of broad peak in 1000–1100 cm^{-1} at Fe_2O_3@SiO_2–SO_3H nanofibers spectra (Figure 5 d) as well as the peaks around 800 cm^{-1} correspond to Si–O–Si [81]. The broad peak that appeared at about 3409 could be shown the stretching of the OH group in the SO_3H moiety [16]. Based on the results of previous studies on Fe_2O_3@SiO_2–SO_3H nanoparticle synthesis, it can be understood that functionalization with SO_3H lead to a wider peak than Fe_2O_3@SiO_2 nanoparticles at about 3400 cm^{-1} [16,23-28]. The same result could be found in Figure 5 by comparing the spectra. The peak at 1631 cm^{-1} represents the physical absorption of the lower amount of water [28]. The peaks of 1089 cm^{-1} and 1384 cm^{-1} are likely hidden under the wide peak at 1000-1400 cm^{-1} that are related to O=S=O stretching vibration in –SO_3H groups [82,83].

Diffraction peaks at around 23.97°, 28.29°, 29.97°, 33.09°, 35.49°, 40.29°, 49.41°, 53.97°, 62.37° and 63.81° which related to the (012), (031), (411), (104), (110), (512), (024), (116), (214) and (300) are readily recognizable from the XRD pattern (Figure 6). The observed diffraction peaks agree well with the structure of Fe_2O_3 (1999 JCPDS file No 24-0072 and 16-0653). It seems that the silica sheath of core-shell nanofibers was in amorph structure without the distinct sharp peak in the XRD pattern. However, the broad peaks at position 10-20° could be assigned to the small amount of silica.

The magnetic properties of Fe_2O_3@SiO_2–SO_3H nanofibers were characterized by a vibrating sample magnetometer (VSM) (Figure 7). The

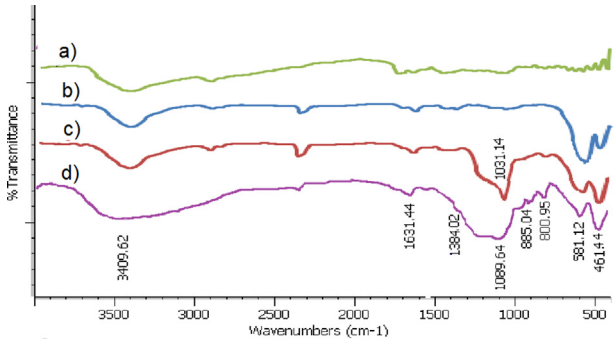

Figure 5. FT-IR spectra of a) PVA/$Fe(NO_3)_3$ nanofiber b) Fe_2O_3 nanofiber c) Fe_2O_3@SiO_2 nanofibers d) Fe_2O_3@ SiO_2–SO_3H nanofibers.

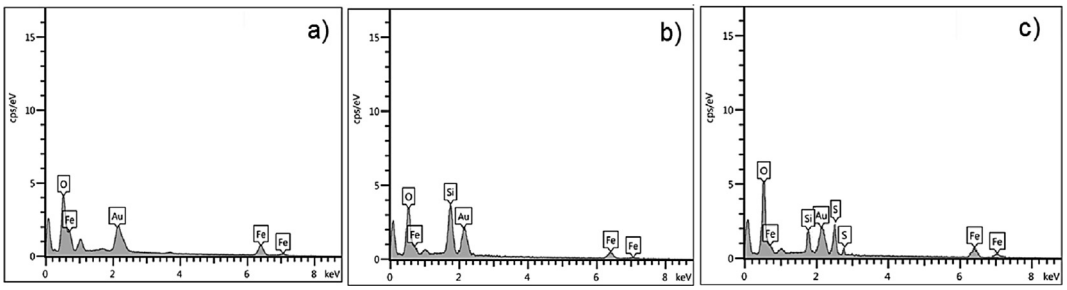

Figure 4. EDS spectra of a) Fe_2O_3 nanofiber b) Fe_2O_3@SiO_2 nanofibers c) Fe_2O_3@SiO_2–SO_3H nanofibers.

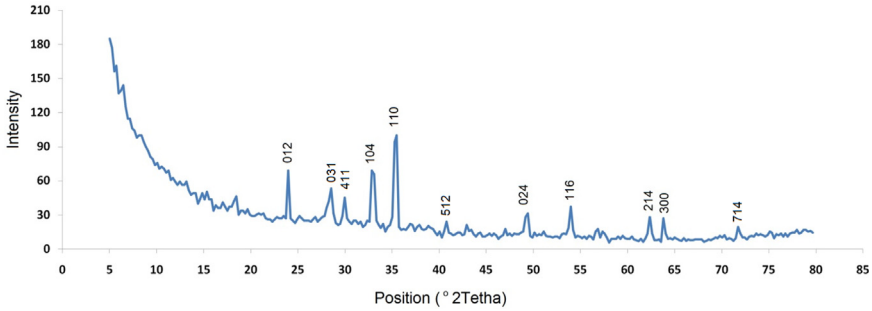

Figure 6. XRD pattern of Fe_2O_3@ SiO_2–SO_3H nanofibers.

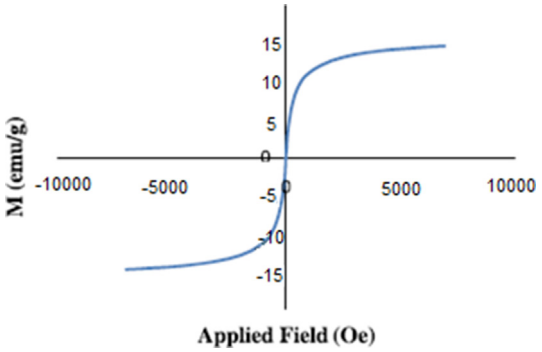

Figure 7. VSM curve of Fe_2O_3@SiO_2–SO_3H nanofibers.

magnetic saturation was about 13.4 emu g^{-1} that is a suitable amount for nanostructure as a magnetic catalyst. The amount of the magnetic saturation of Fe_2O_3@SiO_2–SO_3H nanofibers was very close to the value of Fe_2O_3@SiO_2 nanofibers (14 emu) [46], which can indicate that functionalization with SO_3H had no effects on it. Also, the hysteresis loop was not observed confirming that the catalyst is a super paramagnetic material.

The number of acids functionalized on the surface of core-shell nanofibers was detected using the reverse titration method. It was observed that 0.4 $mmol^{-1}$ g of acid existed in the Fe_2O_3@SiO_2–SO_3H nanofibers that could be enough for catalytic application. The data can be used to specify the meaning of mol% H^+ in catalysts. Mole percent H+ is the percentage of the moles of H+ in proportion to the total number of moles in a mixture. If we use 1mmol of reagent, it is about 0.01 mmol H+ that equals 25 mg Fe_2O_3@SiO_2–SO_3H nanofibers according to the calculation of the number of acids in the surface of Fe_2O_3@SiO_2–SO_3H nanofibers.

3.2. Formamidine catalysis

Although sulfuric acid acts industrially as an effective catalyst, its aqueous environment can interfere with many reactions because many reactants are sensitive to water that can accelerate the rearrangement and production of by-products, reducing the efficiency of the desired reaction. In addition, it can lead to high corrosion in industrial reaction devices. Using catalysts situated on the surface of a mineral solid, such as silica, can be very effective in avoiding the presence of water in the catalyst as well as raising its specific surface area. Core-shell magnetic silica with sulfuric acid as an insoluble, non-corrosive catalyst with high acidity brings ease of working and separation at the end of the reaction by the magnet; it also makes it possible to use it again in a similar reaction without reducing the catalytic power.

Formamidines can be prepared in several ways using different starting materials [15] in most of which toxic solvents are used. High temperature, long reaction time, severe acidity conditions, low yield, hard

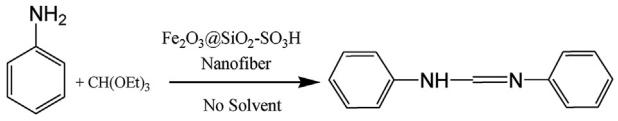

Figure 8. Synthesis of N, N′-diphenylformamidine.

separation and using additional amounts of reactant and catalyst are the problems of these reactions. Triethyl orthoformate is one of the good starting materials that reacts with amines to produce formamidine. In this study, the reaction was done for the first time in acetic acid under reflux at 140–150 °C for 1.5–94 h [23]. The use of liquid acid, high temperature and long reaction time are the three disadvantages of this reaction. Due to the importance of formamidines, the catalytic ability of Fe_2O_3@SiO_2–SO_3H nanofibers in the preparation of formamidines was studied in mild condition and without solvent. For this purpose, the reaction between triethyl orthoformate and aniline was selected as the model reaction (Figure 8).

First, the reaction progress of triethyl orthoformate and aniline at room temperature was followed by thin-layer chromatography in the presence of Fe_2O_3@SiO_2–SO_3H nanofibers. After three hours, the product achieved a yield of 86%. Proper efficiency at low temperature indicates the catalytic activity of Fe_2O_3@SiO_2–SO_3H nanofibers in the direct reaction of formamidine preparation. Next, the effect of an increase in the temperature on the model reaction was investigated (Table 1). The increase in temperature could increase the speed and efficiency of the reaction. The addition of 1 mol% of catalyst at 70 °C synthesized 92 % formamidine during 1 h (Table 1, entry 3). The reaction was remarkably fast. Next, the effect of catalyst amount on the reaction efficiency was investigated. By increasing the amount of catalyst to 3 mol%, the reaction efficiency increased to 96% (Table 1, entry 4). Without a catalyst, no product was prepared at room temperature. At 70 °C, a crystalline amine was formed, but formamidine was not obtained meaning that the reaction needed the catalyst (Table 1, entry 5).

Moreover, the catalytic effect of iron oxide nanofiber with silica coating (Fe_2O_3@SiO_2) was investigated in this reaction (Table 1, entry

Table 1. Optimization of the reaction conditions using the model system.[a]

Entry	Catalyst(mol%)[b]	Temp(°C)	Time (h)	Yield (%)[c]
1	α-Fe_2O_3@SiO_2–SO_3H nanofiber (1)	r.t.	3	86
2	α-Fe_2O_3@SiO_2–SO_3H nanofiber (1)	40	3	90
3	α-Fe_2O_3@SiO_2–SO_3H nanofiber (1)	70	1	92
4	α-Fe_2O_3@SiO_2–SO_3H nanofiber (3)	70	1	96
5	No catalyst	r.t., 70	6	0
6	α-Fe_2O_3@SiO_2 nanofiber (3)	70	4	23

[a] Reaction conditions: triethyl orthoformate (1 mmol), aniline (1 mmol), solvent-free.
[b] mol% H^+ in the catalyst.
[c] Isolated yields.

Table 2. Comparison of catalyst activities.

Entry	Catalyst (mol%) ref.	Temp.(°C)	Time	Yield
1	Fe_2O_3@SiO_2–SO_3H nanofibers (3 mol%)	70	1 h	96
2	Fe_2O_3@SiO_2–SO_3H nanofibers (1 mol%)	r.t.	3 h	86
3	Fe_2O_3@SiO_2-$HCLO_4$ nanoparticles (2.5 mol%) [15]	r.t.	4 h	51
4	Fe_2O_3@SiO_2–HBF_4 nanoparticles (2.5 mol%) [15]	r.t.	4 h	95
5	RH- SO_3H (50 mg) [84]	60	1 min	93
6	Acetic acid [85]	140–160	3–4 h	50–80
7	b-CD (2 mmol) [86]	r.t.	14 h	92

6). By adding the same values of this nanofiber to the reaction and performing it in optimal conditions, it was observed that after four hours, the product was obtained with a yield of 27%, indicating the effectivity of functional group on reaction efficiency, which increased by increasing the acidity of the catalyst surface.

The comparison of the catalytic activity of some catalyst in formamidine synthesis was shown in Table 2. Sheykhan et al. used Fe_2O_3@SiO_2-HA as a magnetic solid acid catalyst to synthesize formamidine (Table 2, entry 3,4) [15]. As observed in Table 2, the yield of reaction was low in the presence of Fe_2O_3@SiO_2-$HCLO_4$ nanoparticles (entry 3); however, better results were achieved with Fe_2O_3@SiO_2–SO_3H nanofibers (entry 1). When Fe_2O_3@SiO_2–HBF_4 nanoparticles (entry 4) were used as catalysts, the yield of reaction exceeded, but the reaction time was still more than Fe_2O_3@ SiO_2–SO_3H nanofibers. It seems that catalysts that are functionalized with SO_3H, such as sulfonated rice husk (RH-SO_3H), had very good results (Table 2, entry 5) but with a difficult catalyst separation process in spite of magnetic catalyst [84]. Archibald et al. synthesized formamidine complex in reflux conditions and low yield of product with acetic acid as a liquid acid catalyst (Table 2, entry 6) [85]. The reaction with cyclodextrin (CD) as a catalyst (Table 2, entry 7) [86] was done at more time (14 h). It was revealed that Fe_2O_3@-SiO_2–SO_3H nanofibers as a novel magnetic catalyst performed this reaction in a shorter time and with higher efficiency. Also, all the above-mentioned studies used more amount of reactant (2 mmol amine) and catalyst (0.05 mmol Fe_2O_3@SiO_2–HBF_4 nanoparticles), but the new procedure of this study included using 1mmol of amine and 0.03 mmol of Fe_2O_3@SiO_2–SO_3H nanofibers.

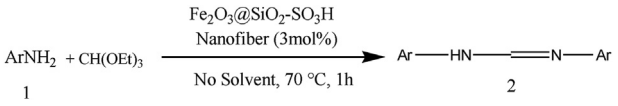

Figure 9. Synthesis of formamidine derivatives.

Finally, the optimum conditions were extended to all types of aniline derivatives. The results of the study revealed that in all cases, high-yield products were obtained and the procedure was applicable in the synthesis of a wide range of formamidine derivatives (Figure 9, Table 3). The reaction in the presence of aniline derivatives was carried out conveniently with the electron donation, withdrawing group and more than one substitution. This method proves to be effective with p-bromoaniline, p-fluoroaniline, 2,4-dichloroaniline and p-nitroaniline as derivatives of aniline with the electron-withdrawing group on the aromatic ring (Table 3, entry 5, 6, 7, 8). As shown in Table 3, the withdrawing electrons groups led to a decrease in efficiency. The yield of reaction with p-bromoaniline was 80% in 3h while the same product achieved in70% in 4h in the presence of Fe_2O_3@SiO_2–HBF_4 nanoparticles [15]. In contrast to

Table 3. Synthesis of formamidine derivatives.[a]

Entry	Amine	product	Time (h)	Melting point (°C)	Yield[b] (%)
1	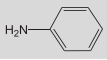	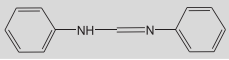	1	136	96
2	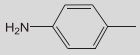	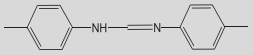	2	139	94
3	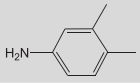	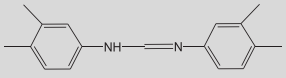	2	162	90
4	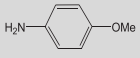	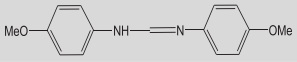	1	95	93
5	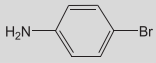	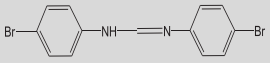	3	169	80
6	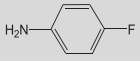	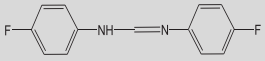	5	142	72
7	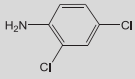	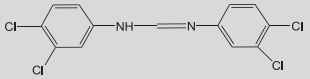	3	135	85
8	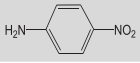	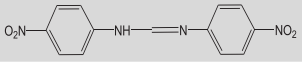	2	201	90
9	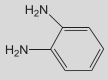	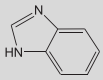	1	170	97
10	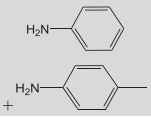	Mixture of product	-	-	-
11		No product	-	-	-

[a] Reaction conditions: triethylorthoformate (1 mmole), aniline (1mmol), solvent-free, α-Fe_2O_3@SiO_2–SO_3H nanofiber (3 mol%), 70 °C.
[b] Isolated yield.

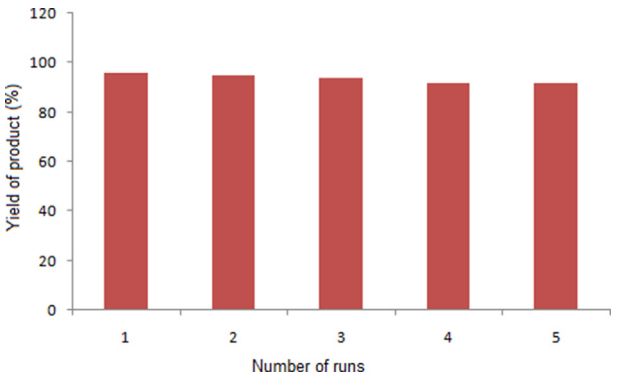

Figure 10. Reusability of Fe_2O_3@SiO_2–SO_3H nanofibers in the reaction of triethyl orthoformate with aniline.

Fe_2O_3@SiO_2–HBF_4 [15] nanoparticles and RH-SO_3H [84], the novel magnetic nanofibers were successful at the synthesis of electron deficient rings such as 2,4-dichloroaniline and p-nitroaniline (Table 3, entry 7,8).

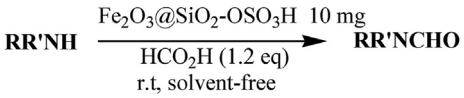

Figure 11. N-formylation of amine derivatives.

To test the possibility of inter-molecular reaction, the reaction of orthophenylenediamine with triethyl orthoformate was done and led to produce benzimidazole in a very high yield (Table 3, entry 9). Among different derivatives of formamidine, benzimidazole had the highest yield due to the high speed of intermolecular reaction. Aiming to prepare unsymmetrical diaryl orthoformamidines, we decided to do a reaction using a mixture of 50:50 mol/mol of aniline and p-toluidine with triethyl orthoformate under the same reaction conditions. The result was a product with 84–86 °C meting point and three new stain in TLC (Table 3, entry 10). It seems that the product is a mixture of unsymmetrical formamidine and two corresponding symmetrical formamidines which is consistent with Robert's finding in the same reaction in the presence of acid [87]. We also tried to synthesize aliphatic formamidine using this procedure. For this purpose, the reaction of t-butyl amine and triethyl orthoformate under the same reaction conditions was examined (Table 3, entry 11). It has been observed in the literature that the formamidines with an aliphatic residue can quickly decompose to the corresponding amines when exposed to silica, and they are less stable than aryl formamidines [88].

The magnetic recycling of catalysts was also investigated. Thus, the reaction between triethyl orthoformate and aniline was studied in the presence of 3 mol% of Fe_2O_3@SiO_2–SO_3H nanofibers at 70 °C during 1h reaction time. After the completion of the reaction, an external magnet was employed to separate the mixture, and recovered Fe_2O_3@SiO_2–SO_3H nanofibers were reused in a subsequent reaction without any significant decrease in activity even after five runs. The isolated product yield decreased slowly from 96% to 92% after five cycles (Figure 10). In

Table 4. The reaction of amines and formic acid that leads to the formamide functional group [a]

Entry	Amine	Product	Time (min)	Melting point (°C)	Yield[b] (%)
1	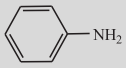	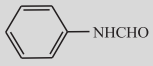	5	47	97
2		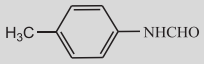	5	52	95
3	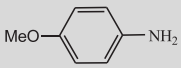	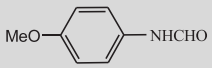	2	79	97
4	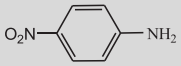	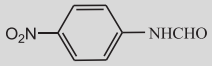	12	194	94
5	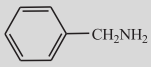	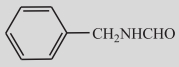	10	60	92
6			15	oil	90
7	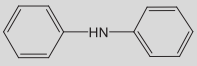	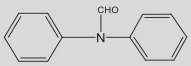	10	71–68	92
8			12	230	96
9	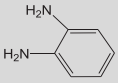	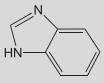	8	170	97
10			5	oil	94
11	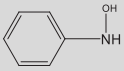	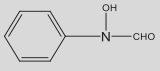	10	149	96

[a] Reaction condition: amine (1mmol), formic acid (1.2 eq), Fe_2O_3@SiO_2–OSO_3H nanofibers (10 mg), room temperature, no solvent.
[b] Separated product yield.

conclusion, we can introduce Fe_2O_3@SiO_2–SO_3H nanofibers as a new and powerful recyclable magnetic catalyst for the conversion of amines to formamidine derivatives under solvent-free conditions. The notable advantages of this catalyst including industrial-scale production, reusability, low-cost separation process of the catalyst by using a magnet and the operational simplicity of the method and its solvent-free condition can present this catalyst as an important alternative to previously reported methods.

3.3. Formamide synthesis

The methods previously used for amine N-formylation [53, 54, 55, 56, 57, 58] have some disadvantages such as high temperature, long reaction time, additional amounts of reactants, the use of reactors, toxic and harmful solvents for the environment, low efficiency and use of expensive and harmful compounds. Because of the importance of the N-formylation reaction and the problems mentioned, the N-formylation reaction of amines was performed in this study using Fe_2O_3@SiO_2–SO_3H nanofiber catalyst and N-formyl products were obtained under room temperature conditions and in short time with high yields.

A variety of amines were used to investigate the magnetic Fe_2O_3@-SiO_2–SO_3H nanofibers catalysis in the formylation reaction (Figure 11) and the results are summarized in Table 4. The formylation of different types of amines, including aliphatic, acyclic, aromatic and heterocyclic compounds, were considered in this study. As shown in Table 4, aromatic amines such as aniline and *p*-toluidine reacted in excellent yields to produce the corresponding *N*-formyl compounds (entries, 1, 2). The most effective result was gained with the amine/formic acid molar ratio of 1–1.2 with 0.01 g of the catalyst at room temperature in solvent-free conditions (Table 4, entry 1,3). The same result can be found in the synthesis of formamide from the N-formylation of amines in the presence of Natrolite zeolite as catalyst [60]. However, more catalyst demand (0.02 g) and hard separation process are the disadvantages of the Natrolite zeolite catalyst. The sterically-hindered amines (entry 6) and poorly reactive ones such as *p*-nitroaniline (entry 4) were easily formylated providing corresponding formamides in good yields. The conversion of *p*-nitroaniline to the corresponding amides was carried out in 94% with Fe_2O_3@SiO_2–SO_3H nanofibers as a catalyst while the yield of reaction was 83% and 90% in the presence of the Natrolite zeolite [60] and RH-SO3H [84] catalysts, respectively. In addition, Nishikawa et al. were not able to do the N-formylation of *p*-nitroaniline probably due to the low acidity of TEOS asa catalyst [65]. It is worth mentioning that the main problem of TEOS is the hard recovery of the liquid catalyst. The method is effective for the formylation of aliphatic amines (entries 6, 8) with high yield. This method can be applied to convert orthophyllen-diamine to benzimidazole in high yields (entry 9) as an inter-molecular reaction. Imidazole as a heterocyclic amine reacted with formic acid with a 94% yield (entry 10). The chemo selectivity of reaction can be seen in the N-formylation of amine functional group in phenyl hydroxyl amine without O-formylation (Entry 11).

The reaction of aniline and formic acid in the presence of Fe_2O_3@-SiO_2–SO_3H nanofibers was used to study the possibility of the magnetic recycling of catalysts. The catalyst was easily separated from the product using an external magnet due to the magnetic properties of the nanofibers. The separated catalysts were applied in the sample reaction over four cycles in high yields.

4. Conclusion

In conclusion, Fe_2O_3@SiO_2–OSO_3H nanofibers were prepared in the following steps: electrospinning, calcinations, coating with silica layer and functionalization with chlorosulfonic acid. The modified, novel, one-dimensional nanostructure was characterized by SEM, TEM, EDS, VSM and FT-IR approving the formation of a core-shell nanofibrous structure. The results revealed that magnetic core-shell nanofibers modified with acid can act as a novel catalyst for the synthesis of formamide and formamidine derivatives with high efficiency. This reaction normally requires high temperature, high acid amount, long reaction conditions and often a difficult catalyst separation process whereas in the method used in this study, most of the above-mentioned disadvantages were removed. The catalyst can be separated by magnet and reused several times in organic reactions without the significant reduction of the yield.

Declarations

Author contribution statement

Hakimeh Ziyadi: Conceived and designed the experiments; Analyzed and interpreted the data; Wrote the paper.

Mitra Baghali: Performed the experiments; Wrote the paper.

Akbar Heydari: Analyzed and interpreted the data; Contributed reagents, materials, analysis tools or data.

Funding statement

This work was supported by Islamic Azad University, Medical Sciences Tehran, Iran (IAUMST).

Data availability statement

Data included in article/supplementary material/referenced in article.

Declaration of interests statement

The authors declare no conflict of interest.

Additional information

No additional information is available for this paper.

Acknowledgements

The authors would like to thank the Active Pharmaceutical Ingredients Research Center (APIRC) and Chemistry Department of Tarbiat Modares University for equipment and laboratory services.

References

[1] N. Diamantopoulos, D. Panagiotaras, D. Nikolopoulos, Comprehensive review on the biodiesel production using solid acid heterogeneous catalysts, J. Thermodyn. Catal. 6 (2015) 143.

[2] F. Liu, X. Ma, H. Li, Y. Wang, P. Cui, M. Guo, H. Yaxin, W. Lu, Sh. Zhou, M. Yu, Dilute sulfonic acid post functionalized metal organic framework as a heterogeneous acid catalyst for esterification to produce biodiesel, Fule 266 (2020) 117149.

[3] P.N.S.M.M. Kamal, N.I. Mohamad, M.E.A. Serit, N.S.A. Rahim, N.I. Jimat, A.S. Alikasturi, Study on the effect of reaction and calcination temperature towards glucose hydrolysis using solid acid catalyst, Mater. Today: Proceedings 31 (2020) 282.

[4] K. Vasić, G. Podrepšek, Ž. Knez, M. Leitgeb, Biodiesel production using solid acid catalysts based on metal oxides, Catalysts 10 (2020) 237.

[5] A.H. Lu, E.L. Salabas, F. Scheuth, Magnetic nanoparticles: synthesis, protection, functionalization, and application, Angew. Chem. Int. Ed. 46 (2007) 1222.

[6] Y. Gao, Bio Functionalization of Magnetic Nanoparticles Biofunctionalization of Nanomaterials, in: C.S. Kumar (Ed.), Wiley-VCH, Winheim, 2005, p. p.72.

[7] M.N. Chen, L.P. Mo, Magnetic nanocatalysts: synthesis and application in multicomponent reactions, Curr. Opin. Green Sustain. Chem. 15 (2019) 27.

[8] C.W. Lim, I.S. Lee, Magnetically recyclable nanocatalyst systems for the organic reactions, Nano Today 5 (2010) 412.

[9] M. Amiri, K. Eskandari, M. Salavati-Niasari, Magnetically retrievable ferrite nanoparticles in the catalysis application, Adv. Colloid Interface Sci. 271 (2019) 101982.

[10] S. Laurent, D. Forge, M. Port, A. Roch, C. Robic, L. Vander Elst, R.N. Muller, Magnetic iron oxide nanoparticles: synthesis, stabilization, vectorization, physicochemical characterizations, and biological applications, Chem. Rev. 108 (2008) 2064.

[11] Q. Sun, X.L. Zhang, Y. Wang, A.H. Lu, Recent progress on core-shell nanocatalysts, Chin. J. Catal. 36 (2015) 683.

[12] Sh. Liu, B. Yu, S. Wang, Y. Shen, H. Cong, Preparation, surface functionalization and application of Fe_3O_4 magnetic nanoparticles, Adv. Colloid Interface Sci. 281 (2020) 102165.

[13] M.B. Gawande, Y. Monga, R. Zboril, R.K. Sharma, Silica-decorated magnetic nanocomposites for catalytic applications, Coord. Chem. Rev. 288 (2015) 118.

[14] M. Kaur, S. Sharma, P.M.S. Bedi, Silica supported Brönsted acids as catalyst in organic transformations: a comprehensive review, Chin. J. Catal. 36 (2015) 520.

[15] M. Sheykhan, M. Mohammadquli, A. Heydari, A new and green synthesis of formamidines by c-Fe2O3@SiO2–HBF4 nanoparticles as a robust and magnetically recoverable catalyst, J. Mol. Struct. 1027 (2012) 156.

[16] K. Rajkumari, J. Kalita, D. Das, L. Rokhum, Magnetic Fe_3O_4@silica sulfuric acid nanoparticles promoted regioselective protection/deprotection of alcohols with dihydropyran under solvent-free conditions, RSC Adv. 7 (2017) 56559.

[17] A. Zare, N. Lotfifar, M. Dianat, Preparation, characterization and application of nano-[Fe3O4@-SiO2@R-NHMe2][H2PO4] as a novel magnetically recoverable catalyst for the synthesis of pyrimido[4,5-b]quinolines, J. Mol. Struct. 1211 (2020) 128030.

[18] F. Nemati, R. Saeedi rad, Nano-Fe_3O_4 encapsulated-silica particles bearing sulfonic acid groups as a magnetically separable catalyst for green and efficient synthesis of functionalized pyrimido[4,5-b]quinolines and in deno fused pyrido[2,3-d] pyrimidines in water, Chin. Chem. Lett. 24 (2013) 370.

[19] G. Mohammadi Ziarani, N. Lashgari, A. Badiei, Sulfonic acid-functionalized mesoporous silica (SBA-Pr-SO3H) as solid acid catalyst in organic reactions, J. Mol. Catal. A: Chem. 397 (2015) 166.

[20] P. Wang, Y. Zhao, J. Liu, Versatile design and synthesis of mesoporous sulfonic acid catalysts, Sci. Bull. 63 (2018) 252.

[21] Y. Lei, M. Zhang, G. Leng, C. Ding, Y. Ni, SO3H-functionalized porous organic polymer with amphiphilic and swelling properties: a highly efficient solid acid catalyst for organic transformations in water, Microporous Mesoporous Mater. 299 (2020) 110110.

[22] H. Kefayati, M. Golshekan, S. Shariati, M. Bagheri, Fe_3O_4@MCM-48–SO_3H: an efficient magnetically separable nanocatalyst for the synthesis of benzo[f]chromeno [2,3-d]pyrimidinones, Chin. J. Catal. 36 (2015) 572.

[23] A. Kundu, S. Mukherjee, A. Pramanik, Synthesis of a new class of pyrazole embedded spirocyclic scaffolds using magnetically separable Fe_3O_4@SiO_2–SO_3H nanoparticles as recyclable solid acid support, RSC Adv. 5 (2015) 107847.

[24] J. Safaei-Ghomi, R. Aghagoli, H. Shahbazi-Alavi, Synthesis of hexahydro-4-phenylquinoline-3-carbonitriles using Fe_3O_4@SiO_2-SO_3H nanoparticles as a superior and retrievable heterogeneous catalyst under ultrasonic irradiations, Z. Naturforsch. 73 (2018) 269.

[25] J. Safaei-Ghomi, H. Shahbazi-Alavi, A flexible one-pot synthesis of pyrazolopyridines catalyzed by Fe_3O_4@SiO_2-SO_3H nanocatalyst under microwave irradiation, Sci. Iran. 24 (2017) 1209.

[26] A. Kiasat, J. Davarpanah, Fe_3O_4@Silica sulfuric acid core–shell composite as a novel nanomagnetic solid acid: synthesis, characterization and application as an efficient and reusable catalyst for one-pot synthesis of 3,4-dihydropyrimidinones/thiones under solvent-free conditions, Res. Chem. Intermed. 41 (2013) 2991.

[27] L. Sadighnia, B. Zeynizadeh, S. Karami, M. Abdollahi, Nano-Fe_3O_4@SiO_2-SO_3H: a magnetic, reusable solid-acid catalyst for solvent-free reduction of oximes to amines with the NaBH3CN/ZrCl4 system,, J. Chin. Chem. Soc. 66 (2018) 535.

[28] Z. Shahedi, Y. Mansoori, Fe_3O_4@SiO_2-SO_3H Nanoparticles: an efficient magnetically retrievable catalyst for esterification reactions, J. Particle Sci. Technol. 2 (2018) 67.

[29] V. Shabafrooz, M. Mozafari, D. Vashaee, L. Tayebi, Electrospun nanofibers: from filtration membranes to highly specialized tissue engineering scaffolds, J. Nanosci. Nanotechnol. 14 (2014) 522.

[30] H. Chen, M. Huang, Y. Liu, L. Meng, M. Ma, Functionalized electrospun nanofiber membranes for water treatment: a review,, Sci. Total Environ. 739 (2020) 139944.

[31] P.P. Mane, R.S. Ambekar, B. Kandasubramanian, Electrospun nanofiber-based cancer sensors: a review,, Int. J. Pharm. 583 (2020) 119364.

[32] T.S.M. Kumar, K.S. Kumar, N. Rajini, S. Siengchin, N. Ayrilmis, A.V. Rajulu, A comprehensive review of electrospun nanofibers: food and packaging perspective, Composites Part B 175 (2019) 107074.

[33] H.M. Ibrahim, A. Klingner, A review on electrospun polymeric nanofibers: production parameters and potential applications,, Polym. Test. 90 (2020) 106647.

[34] S. Thenmozhi, N. Dharmaraj, K. Kadirvelu, H.Y. Kim, Electrospun nanofibers: new generation materials for advanced applications, Mater. Sci. Eng. B 217 (2017) 36–48.

[35] H. Esfahani, R. Jose, S. Ramakrishna, Electrospun Ceramic Nanofiber Mats Today: Synthesis, Properties, and Applications, Materials 10 (2017) 1238.

[36] Y. Dai, W. Liu, E. Formo, Y. Sun, Y. Xia, Ceramic nanofibers fabricated by electrospinning and their applications in catalysis, environmental science, and energy technology, Polym. Adv. Technol. 22 (2011) 326–338.

[37] A.L. Monaca, A. Paolella, A. Guerfi, F. Rosei, K. Zaghib, Electrospun ceramic nanofibers as 1D solid electrolytes for lithium batteries, Electrochem. Commun. 104 (2019) 106483.

[38] L.A. Mercante, R.S. Andre, L.H.C. Mattoso, D.S. Correa, Electrospun ceramic nanofibers and hybrid-nanofiber composites for gas sensing, ACS Appl. Nano Mater 2 (2019) 4026–4042.

[39] Z. Li, S. Liu, S. Song, W. Xu, Y. Sun, Y. Dai, Porous ceramic nanofibers as new catalysts toward heterogeneous reactions, Compos. Commun. 15 (2019) 168–178.

[40] Y. Dai, E. Formo, H. Li, J. Xue, Y. Xia, Surface-functionalized electrospun titania nanofibers for the scavenging and recycling of precious metal ions, Chem. Sus Chem. 9 (2016) 2912–2916.

[41] S.R. Hosseini, S. Ghasemi, M. Kamali-Rousta, Preparation of CuO/NiO compositenanofibers by electrospinning and their application for electro-catalytic oxidation of hydrazine, J. Power Sources 343 (2017) 467–476.

[42] Y. Zheng, H. Chen, Y. Dai, N. Zhang, W. Zhao, S. Wang, Y. Lou, Y. Li, Y. Sun, Preparation and characterization of Pt/TiO2 nanofibers catalysts for methanol electro-oxidation, Electrochim. Acta 178 (2015) 74–79.

[43] Y. Dai, Y. Chai, Y. Sun, W. Fu, X. Wang, Q. Gu, T.H. Zeng, Y. Sun, New versatile Pt supports composed of graphene sheets decorated by Fe2O3 nanorods and N-dopants with high activity based on improved metal/support interactions, J. Mater. Chem. 3 (2015) 125–130.

[44] H. Ziyadi, A. Heydari, F. Nikbakht, Magnetic α-Fe2O3 nanofibers: an efficient and recyclable catalyst for solvent free selective oxidation of benzylic alcohols, Lett. Org. Chem. 12 (2015) 598.

[45] E. Ghasemi, H. Ziyadi, A. Moein Afshar, M. Sillanpä, Iron oxide nanofibers: a new magnetic catalyst for azo dyes degradation in aqueous solution,, Chem. Eng. J. 264 (2014) 146–151.

[46] H. Ziyadi, A. Heydari, S. Mahdi Rezayat, Preparation and characterization of magnetic α-Fe_2O_3 nanofibers coated with uniform layers of silica, Ceram. Int. 40 (2014) 5913.

[47] H. Ziyadi, A. Heydari, Core–shell a-Fe_2O_3@SiO_2 nanofibers: a magnetic recyclable catalyst for one-pot reductive amination of carbonyl compound,, Catal. Lett. 144 (2014) 2210.

[48] Y. Han, L. Cai, An efficient and convenient synthesis of formamidines, Tetrahedron Lett. 38 (1997) 5423.

[49] S.K. Guchhait, G. Priyadarshani, V. Chaudhary, D.R. Seladiya, T.M. Shah, N.P. Bhogayta, One-pot preparation of isocyanides from amines and their multicomponent reactions: crucial role of dehydrating agent and base, RSC Adv. 3 (2013) 10867.

[50] I.M. Downie, M.J. Earle, H. Heaney, K.F. Shuhaibar, Vilsmeier formylation and glyoxylation reactions of nucleophilic aromatic compounds using pyrophosphoryl chloride, Tetrahedron 49 (1993) 4015.

[51] A. Jackson, O. Meth-Cohn, A new short and efficient strategy for the synthesis of quinolone antibiotics, J. Chem. Soc. Chem. Commun (1995) 1319.

[52] B.C. Chen, M.S. Bednarz, R. Zhao, J.E. Sundeen, P. Chen, Z. Shen, A.P. Skoumbourdis, J.C. Barrish, A new facile method for the synthesis of 1-arylimidazole-5-carboxylates, Tetrahedron Lett. 41 (2000) 5453.

[53] R. Luo, X. Lin, J. Lu, X. Zhou, H. Ji, Zinc, Zinc phthalocyanine as an efficient catalyst for halogen free Synthesis of formamides from amines via carbon dioxide hydrosilylation under mild conditions, Chin. J. Catal. 38 (2017) 1382.

[54] H. Liu, Q. Mei, Q. Xu, J. Song, H. Liu, B. Han, Synthesis of formamides containing unsaturated groups by N formylation of amines using CO_2 with H_2, Green Chem. 19 (2017) 196.

[55] S. Hun Kwak, Y.D. Gong, Unexpected route for the synthesis of N,N-dialkyl formamidines using phenyl chloroformate and N,N-dialkyl formamides, Tetrahedron 69 (2013) 7107.

[56] J. Deutsch, R. Eckelt, A. Kö ckritz, A. Martin, Catalytic reaction of methyl formate with amines to formamides, Tetrahedron 65 (2009) 10365.

[57] P.G. Reddy, G.D.K. Kumar, S. Baskaran, A convenient method for the N-formylation of secondary amines and anilines using ammonium formate, Tetrahedron Lett. 41 (2000) 9149.

[58] P. Strazzolini, A.G. Giumanini, S. Cauci, Acetic formic anhydride a review, Tetrahedron 40 (1990) 1081.

[59] B. Das, K. Meddeboina, P. Balasubramanayam, V.D. Boyapati, K.D. Nandan, A remarkably simple N-formylation of anilines using polyethylene glycol,, Tetrahedron Lett. 49 (2008) 2225.

[60] D. Habibi, M. Nasrollahzadeh, H. Sahebekhtiari, Green synthesis of formamides using the Natrolite zeolite as a natural, efficient and recyclable catalyst, J. Mol. Catal. A: Chem. 378 (2013) 148.

[61] M. Hosseni-Sarvari, H. Sharghi, ZnO as a new catalyst for N-formylation of amines under solvent-free conditions, J. Org. Chem. 71 (2006) 6652.

[62] D. Wei, C. Cui, Z. Qu, Y. Zhu, M. Tang, A computational study on the reaction mechanisms of N-formylation of amines under a Lewis acid catalysis, J. Mol. Struct.: THEOCHEM 951 (2010) 89.

[63] M. Lei, L. Ma, L. Hua, A convenient one-pot synthesis of formamide derivatives using thiamine hydrochloride as a novel catalyst, Tetrahedron Lett. 51 (2010) 4186.

[64] Y. Zhang, P. Cao, H.Y. Zhang, G. Yin, J. Zhao, Cobalt nanoparticles anchoring on nitrogen doped carbon with excellent performances for transfer hydrogenation of nitrocompounds to primary amines and N-substituted formamides with formic acid, Catal. Commun. 129 (2019) 105747.

[65] Y. Nishikawa, H. Nakamura, N. Ukai, W. Adachi, O. Hara, Tetraethylorthosilicate as a mild dehydrating reagent for the synthesis of N-formamides with formic acid, Tetrahedron Lett. 58 (2017) 860.

[66] S.M. Hashemi, A. Yahyazadeh, N. Nami, Synthesis of novel 6-Cyano-9-(aryl)-9H-purineDerivatives via formamidine intermediates, E-J. Chem. 9 (2012) 219.

[67] A.S. Kumar, J. Kudva, M. Lahtinen, A. Peuronen, R. Sadashiva, D. Naral, Synthesis, characterization, crystal structures and biological screening of 4-amino quinazoline sulfonamide derivatives, J. Mol. Struct. 1190 (2019) 29.

[68] S.D. Oladipo, B. Omondi, C. Mocktar, Synthesis and structural studies of nickel(II)- and copper(II)-N,N0- diarylformamidine dithiocarbamate complexes as antimicrobial and antioxidant agents, Polyhedron 170 (2019) 712.

[69] W. Hsu, X.K. Yang, P.M. Chhetri, S.J. Lin, Y.S. Li, T.R. Chen, J.D. Chen, Au(I) and Ag(I) formamidinate tetranuclear complexes and coordination polymers: synthesis, structures and luminescent properties, Inorganica Chimica Acta 482 (2018) 785.

[70] A.A. Soliman, M.A. Amin, A.M. Sayed, A.A.A. Abou-Hussein, W. Linert, Cobalt and copper complexes with formamidine ligands: synthesis, crystal X-ray study, DFT calculations and cytotoxicity, Polyhedron 161 (2019) 213.
[71] E.D. Akpan, S.O. Ojwach, B. Omondi, V.O. Nyamori, Zn(II) and Cu(II) formamidine complexes: structural, kinetics and polymer tacticity studies in the ring-opening polymerization of e-caprolactone and lactides, New J. Chem. 40 (2016) 3499.
[72] A.A. Soliman, O.I. Alajrawy, F.A. Attaby, W. Linert, New binary and ternary platinum(II) formamidine complexes: synthesis, characterization, structural studies and in-vitro antitumor Activity, J. Mol. Struct. 1115 (2016) 17.
[73] A.Y. Khormi, T.A. Farghaly, M.R. Shaaban, Pyrimidyl formamidine palladium (II) complex as a nanocatalyst for aqueous Suzuki-Miyaura coupling, Heliyon 5 (2019) 1367.
[74] I. Tamm, Ribonucleic acid synthesis and influenza virus multiplication, Science 126 (1957) 1235.
[75] A.R. Porcari, R.V. Devivar, L.S. Kucera, J.C. Drach, L.B. Townsend, Design, synthesis, and antiviral evaluations of 1-(substituted benzyl)-2-substituted-5,6-dichlorobenzimidazoles as nonnucleoside analogues of 2,5,6-trichloro-1-(beta-D-ribofuranosyl)benzimidazole, J. Med. Chem. 41 (1998) 1252.
[76] S.M. Sondhi, M. Dinodia, A. Kumar, Synthesis, anti-inflammatory and analgesic activity evaluation of some amidine and hydrazone derivatives, Bioorg. Med. Chem. 14 (2006) 4657.
[77] P. Sienkiewich, K. Bielawski, A. Bielawska, J. Palka, Inhibition of collagen and DNA biosynthesis by a novel amidine analogue of chlorambucil is accompanied by deregulation of β1-integrin and IGF-I receptor signaling in MDA-MB 231 cells, Environ. Toxicol. Pharmacol. 20 (2005) 118.
[78] T.M. Sielecki, J. Liu, S.A. Mousa, A.L. Racanelli, E.A. Hausner, R.R. Wexler, R.E. Olson, Synthesis and pharmacology of modified amidine isoxazoline glycoprotein IIb/IIIa receptor antagonists, Bioorg. Med. Chem. Lett 11 (2001) 220.
[79] C.E. Stephens, E. Tanious, S. Kim, D.W. Wilson, W.A. Schell, J.R. Perfect, S.G. Franzblau, D.W. Boykin, Diguanidino and "Reversed" Diamidino 2,5-Diarylfurans as antimicrobial agents, J. Med. Chem. 44 (2001) 1741.
[80] W. Zheng, Z. Li, H. Zhang, W. Wang, Y. Wang, C. Wang, Electrospinning route for a-Fe2O3 ceramic nanofibers and their gas sensing properties, Mater. Res. B 44 (2009) 1432.
[81] M.I. Barrena, J.M.G. Salazar, A. Soria, L. Matesanz, Pre-hydrolysed ethyl silicate as an alternative precursor for SiO_2-coated carbon nanofibers, Appl. Surf. Sci. 258 (2011) 1212.
[82] S. Wang, L. Lyu, G. Sima, Y. Cui, B. Li, X. Zhang, L. Gan, Optimization of fructose dehydration to 5-hydroxymethylfurfural catalyzed by SO3H-bearing lignin-derived ordered mesoporous carbon, Kor. J. Chem. Eng. 36 (2019) 1042–1050.
[83] F. Poch, Access aux alkyl (ou aryl)-4 diamino-3,6 pyrazolo [3,4-b], Tetrahedron 42 (1986) 4461–4469.
[84] M. Seddighi, F. Shirini, M. Mamaghani, An efficient method for the synthesis of formamidine and formamide derivatives promoted by sulfonated rice husk ash (RHA SO_3H), J. Iran chem. For. Soc. 12 (2015) 433.
[85] J. Archibald, N.W. Alcock, D.H. Busch, D.R. Whitcomb, Synthesis and characterization of functionalized N,N'-Diphenylformamidinate Silver(I) Dimers: solid-state structures and solution properties, Inorg. Chem. 38 (1999) 5571.
[86] D.R. Patil, D.S. Dalal, Biomimetic approach for the synthesis of N, N-diarylsubstituted formamidines catalyzed by b-cyclodextrin in water, Chin. Chem. Lett. 23 (2012) 1125.
[87] R.M. Roberts, Ortho Esters, Imidic Esters and Amidines. The identity of N-phenyl-N'-p-tolylformamidine, J. Am. Chem. Soc. 72 (1950) 3603.
[88] A. Porcheddu, G. Giacomelli, I. Piredda, Parallel synthesis of trisubstituted formamidines: a facile and versatile procedure, J. Comb. Chem. 11 (2009) 126.